DOI: 10.4149/BLL_2023_024

Bratisl Med J 2023; 124 (2)
151 – 157

CLINICAL STUDY

Malate reduced kidney injury molecule (KIM-1) expression and selectively upregulated the renal nitric oxide production in obstructive nephropathy

Osaze EDOSUYI[1,3], Myung CHOI[3], Vashti EDOSUYI[2], Ighodaro IGBE[1], Adebayo OYEKAN[3]

Department of Pharmacology & Toxicology, Faculty of Pharmacy, University of Benin, Ugbowo, Benin city, Nigeria.
osaze.edosuyi@uniben.edu

ABSTRACT
BACKGROUND: Malate, the tricarboxylic acid (TCA) cycle intermediary, upregulates renal nitric oxide (NO) signaling, and NO is renoprotective in nephropathy.
OBJECTIVES: This study explored the hypothesis that malate could increase renal NO and decrease renal injury and fibrotic markers in obstructive nephropathy.
METHODS: Kidney injury was induced in rats via unilateral surgical ligation of the ureter, there after, rats were treated with malate (600 mg/kg, p.o.) for ten days. Urine was collected on days 0, 4, 7 and 10. Urinary sodium excretion was also determined. Western blot and biochemical analyses were carried on the nephropathic kidneys.
RESULTS: Malate reduced kidney injury molecule (KIM-1) expression in the renal cortex and medulla of nephropathic rats ($p < 0.05$). NO production was selectively increased in the medulla of nephropathic rats treated with malate (58.3±1.3 vs 77.8±4.4 μM/ng, $p < 0.05$). Superoxide dismutase and catalase activity increased in the kidney of malate-treated nephropathic rats ($p < 0.05$). Transforming growth factor (TGF-β), an index of fibrosis, increased in the cortex but not medulla of the malate-treated UUO group. There was a consistent increase in collagenase activity in the cortex, and a reduction in the medulla.
CONCLUSION: Malate ameliorated the injury and inflammation but selectively reduced fibrosis in obstructive nephropathy *(Fig. 6, Ref. 32)*. Text in PDF *www.elis.sk*
KEY WORDS: Malate, tricarboxylic acid cycle, nitric oxide, kidney injury molecule (KIM-1), obstructive nephropathy.

Introduction

Obstructive nephropathy is one of the frequent causes of kidney injury (1). Obstructive nephropathy is surgically induced in the laboratory via unilateral ureter obstruction (UUO) (2). The unilateral ureter obstruction (UUO) is a unique model that presents a viable tool for assessing pathologies associated with both acute kidney injury (AKI) and chronic kidney disease (CKD)(3). CKD has become a disease of importance due to its rising prevalence and devastating outcomes (4).

The obstruction of the ureter leads to an acute kidney injury and progressive fibrosis, which eventually depresses renal function (Takaori and Yanagita, 2016). The UUO model is underlined by tubular apoptosis, oxidative stress, renal fibrosis, and inflammation that eventually lead to cell death and irreversible renal damage (Martínez-Klimova et al, 2019). There is also an upregulation in gene markers such as kidney injury molecule (KIM-1) and transforming growth factor (TGF-β) (7). The dysfunction in urinary flow causes increased intrarenal pressure and decreased renal blood flow that leads to renal injury (Song et al, 2019). Recently, malate, the tricarboxylic acid (TCA) cycle intermediary has been reported to restore renal blood flow via an increase in nitric oxide (NO) production (9). NO increases renal blood flow and has an ameliorative and renoprotective role in nephropathy (10). Hence, it is possible that malate may improve pathological outcomes in nephropathy due to its link to NO signaling.

This study assessed the possibility that malate could modulate nitric oxide production in obstructive nephropathy, reduce renal fibrotic markers and inflammation that ameliorate kidney injury and eventually improve renal outcomes in both AKI and CKD.

[1]Department of Pharmacology & Toxicology, Faculty of Pharmacy, University of Benin, Benin city, Nigeria, [2]Department of Child Health, University of Benin Teaching Hospital, Benin City, Nigeria, and [3] Center for Cardiovascular Diseases, Gray Hall Suites College of Pharmacy & Health Sciences Texas Southern University, Houston, Texas, USA

Address for correspondence: Osaze EDOSUYI, PharmD, PhD, Department of Pharmacology & Toxicology, Faculty of Pharmacy, University of Benin, PMB 1154, Ugbowo, Benin city, Nigeria.
Phone: +2348025228545

Acknowledgement: This work received grant support from the National Institutes of health (NIH) (5G12 MD007605), USA.

Materials and methods

Animals

Male Sprague Dawley rats (150–350 g, Harlan Sprague Dawley, Houston, TX) were housed in the well-ventilated animal facility of Texas Southern University, Houston, Texas and under a 12-hour

lightning-controlled condition. The animals were bred in standard cages, kept on rat pelletized feed (Purina Chow; Purina, St Louis MO, USA) and had free access to water. All Experiments were aligned with the Care and Use of Laboratory Animals guidelines of the National Institutes of Health. The Institutional Animal Care and Use Committee (IACUC) of Texas Southern University, Houston, Texas, approved protocols for this study (Protocol #9004/Rats/1034).

Unilateral ureter obstruction (UUO) procedure

Animals were anaesthetized with ketamine + xylazine (100 mg/kg, i.p). The left side of the abdomen was shaved with an electric clipper and cleaned with 1 % chlorhexidine and 70 % alcohol. A left-sided laparotomy carefully exposed the left ureter that was ligated using a 7/0 sterilized silk thread. The incision was stitched with absorbable plain gut suture (6/0), and the outer skin was covered with 9 mm sterilized wound clips. A 24-h recovery period was allowed before drug administration commenced. The procedure was the same in sham-grouped animals except the animals did not undergo ureter ligation (11). The animals were randomly divided into three (3) groups having eight (8) animals, each as follows: Group I: Sham (distilled water, 3 mL/kg, p.o.), group II: UUO (distilled water, 3 mL/kg p.o.) and group III: UUO + Malate (600 mg/kg, p.o.). The animals were placed in metabolic cages and treated daily for 10 days. 24-h urine was collected by gravimetry on days 0, 4, 7 and 10. The animals were euthanized on the last day, and the heart and kidneys were excised and immediately frozen with liquid nitrogen, weighed, and stored at -80° C for biochemical and western blot analyses. The isolated kidneys were separated into cortex and medulla using a sterilized scalpel. Tissue homogenization and protein quantification assays of the cortex and medulla were performed as previously described (12).

Urinary protein quantification (UprotV)

The collected urine was assayed for urine using procedures stated in the Biorad® protein assay kit. Briefly, urine samples (0.02 mL) were mixed with 0.08 mL of distilled water. 0.01 mL of the diluted urine samples were mixed with 0.990 mL of Biorad reagent®. Albumin (0.125, 0.250, 0.5, 1 and 2 mg/mL) were prepared and subjected to the same procedure. The absorbances of the urine samples and albumin were determined at 595 nm.

Urinary sodium (UNaV) assay

The sodium content of the collected urine samples was quantified using flame photometry (13). Briefly, 0.5 mL of urine sample was added to 4.5 mL of distilled water. Sodium chloride was prepared at the following concentrations: 1, 5, 10, 25, 50, 100 and 200 mM. The emitted light intensity of the urine samples and standard sodium chloride was measured at 589 nm against a reagent (distilled water).

Collagenase assay

The assay was modified and carried out as described (14). Briefly, 200 mg of cortex or medulla was weighed into clean glass bottles and incubated at 65 °C in a dry oven for 18 hours. After incubation, 5 ml of 6M HCL was added, and samples were placed in a heating block at 110 °C for 18 hours. This was followed by the addition of 2.5 mL of distilled water. The resulting mixture was kept at room temperature for 10 minutes before the withdrawal of 1 mL of supernatant which was pipetted into clean glass tubes. Samples in the glass tubes were neutralized by the addition of 0.3 mL of 5M NaOH and 0.7 mL of distilled water. After vortexing, 0.4 mL of tissue supernatant was withdrawn from glass tubes and 0.1 mL of 70 % isopropanol was added. A developer solution was prepared by mixing chloramine T in acetate buffer (1 : 4). Tissue supernatant (0.5 mL) from glass tubes was mixed with 0.5 mL of Chloramine T in acetate buffer (developer solution) and incubated at room temperature for 20 minutes. After incubation, 0.5 mL of Erlich's solution was added to tissue supernatant and the reaction mixture was incubated at 60 °C in a water bath for 30 minutes. Samples were kept at room temperature and read at 558 nm.

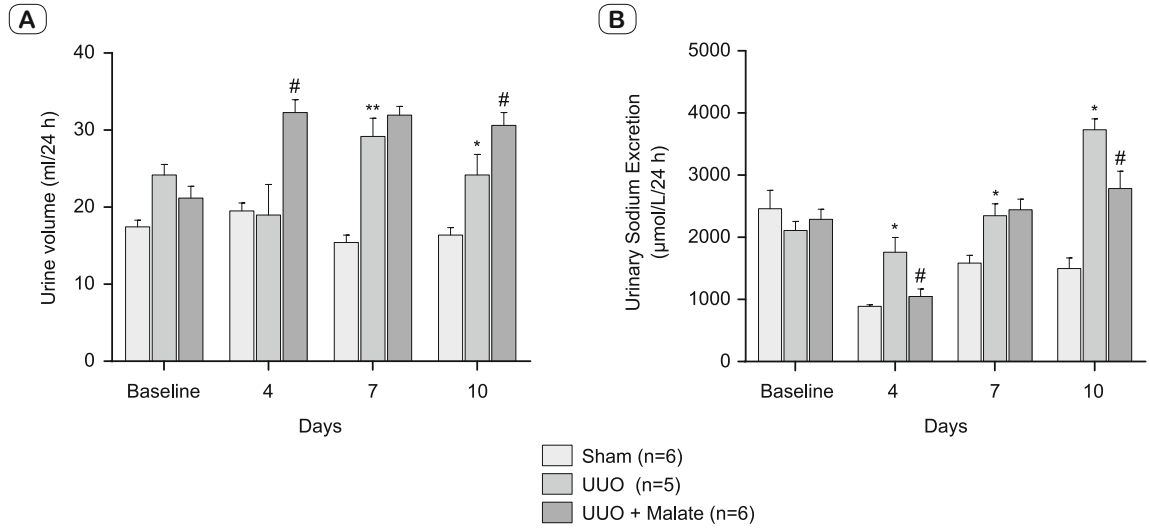

Fig. 1. Urine output (A) and sodium excretion (B) in nephropathic rats treated with malate (600 mg/kg, po) for 10 days. * p < 0.05, ** p < 0.01, compared to sham-operated group. # p < 0.05 compared to UUO group. Unilateral Ureter obstruction (UUO).

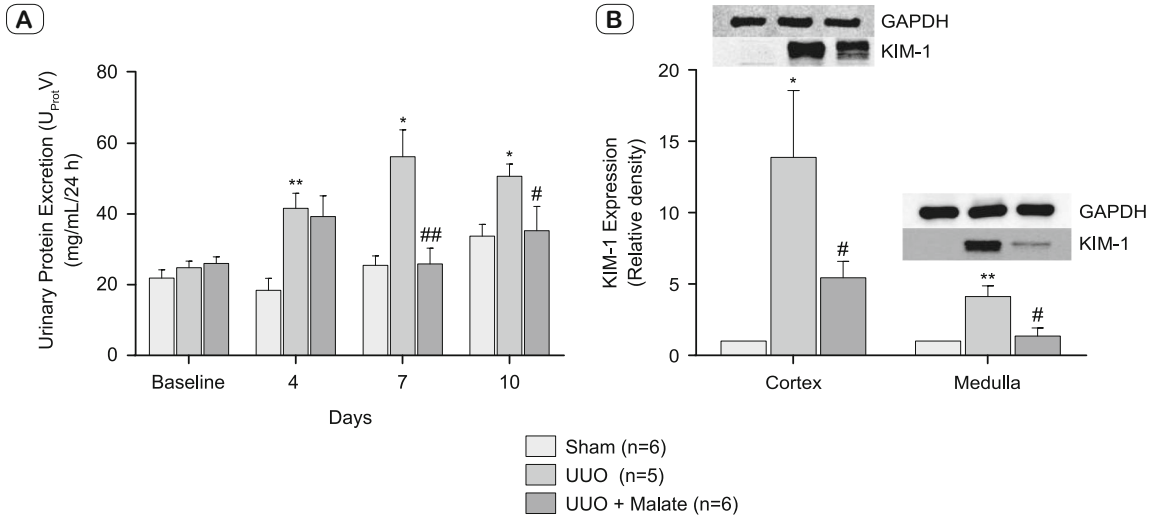

Fig. 2. Proteinuria (A) and kidney injury molecule (KIM-1) expression (B) in rats with UUO-induced nephropathy treated with malate (600 mg/kg, p.o.) for 10 days. * p < 0.05, ** p < 0.01 vs sham group. # p < 0.05, ## p < 0.01, compared to UUO group. Unilateral Ureter obstruction (UUO).

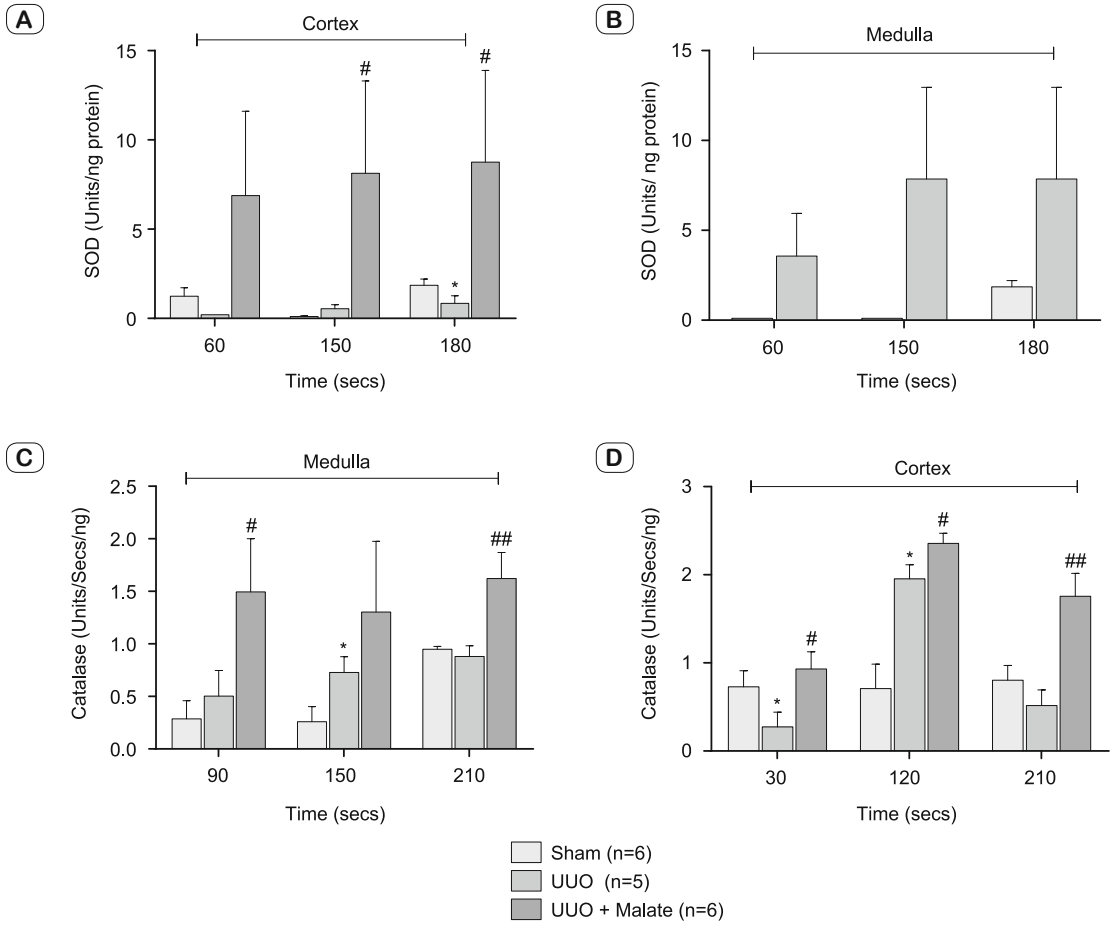

Fig. 3. Effect of malate (600 mg/kg, p.o.) on renal superoxide dismutase (A & B) and catalase activities (C & D) in obstructive nephropathy. * p < 0.05, compared to sham. # p < 0.05, ## p < 0.01vs UUO group. Unilateral Ureter obstruction (UUO). p < 0.05) (Fig. 4B).

Nitric oxide assay

Nitric oxide in the homogenized renal cortex/medulla was quantified using the modified procedure of (15). Briefly, 0.5 mL of homogenate was added to 0.5 mL of Griess reagent (1 g sulphanilamide + 100 mg of N-(-1-naphthyl) ethylenediamine (NEDD). Sodium nitrite ($NaNO_2$) (1, 2, 5, 10 and 20 µM) was prepared and subjected to the same procedure. The sample/standard mixtures were immediately read at 540 nm against a blank solution (0.5 mL of distilled water + 0.5 mL of Griess reagent).

Arginase assay

Arginase was quantified in the homogenized renal cortex/medulla using the method of (16). Briefly, 40 µg of homogenate was mixed with 1 M of magnesium chloride (MgCL2) at 37 °C for 30 minutes. The mixture was further mixed with 0.5 mL of L-arginine buffered solution at 37 °C for 1 hour. After incubation, a developer solution containing 0.05 mL of Ninhydrin + 0.45 mL of acetic acid + 0.05 mL of phosphoric acid solution was added and the mixture was heated at 95 °C for 1 hour. The resulting mixture was cooled and read at 530 nm against a reagent blank containing, 0.01 mL of 1 M magnesium chloride + 0.49 mL of L-Arginine buffer + 0.5 mL of developer solution.

Superoxide dismutase and catalase assays

Catalase and superoxide dismutase (SOD) assays were carried out as previously described (17, 18).

Western blot analyses

Blotting was carried out as previously described (12). Kidney injury molecule (KIM- 1) antibody was purchased from R&D systems (Minneapolis, USA), transforming growth factor (TGF-β) antibody and nuclear factor erythroid 2-related factor 2 (Nrf2) was sourced from Abcam (Massachusetts, USA).

Statistical analysis

Results are expressed as mean±SEM. Data analysis was performed using a one-way analysis of variance (ANOVA) followed by Dunnett's post-hoc test. Graph pad Prism software was used for analysis and $p < 0.05$ was considered significant.

Results

Effect of malate on urine output and sodium excretion in UUO-induced nephropathy

As shown in Figure 1a, urine output in the UUO group significantly increased on days 7 and 10 above vehicle-treated (sham) levels ($p < 0.05$). Malate increased urine output in UUO-induced renal injury, exerting a peak increase on day 4 (18.9±3.9 vs 32.2±1.7 mL, $p < 0.01$). There was a stepwise increase in sodium excretion in the UUO group all through the experiment vs sham ($p < 0.05$) (Fig. 1b). Treatment with malate significantly reduced sodium excretion on days 4 (1761±237.2 vs 1049±118.4 µmol/L) and 7 (3730±175 vs 2784±282 µmol/L), compared to the UUO group (Fig. 1b).

Malate reduced renal kidney injury molecule (KIM-1) expression and proteinuria in obstructive nephropathy

KIM-1, an index of kidney injury, was significantly elevated in the cortex and the medulla of rats with UUO-induced nephropathy when compared to the sham group ($p < 0.05$) (Fig. 2b). Malate reduced KIM 1 expression in the renal cortex (60 %) and medulla (68 %) of the UUO group ($p < 0.05$). Similarly, proteinuria in UUO rats significantly increased in a time-dependent manner when compared to the sham group ($p < 0.05$) (Fig. 2a). Malate exerted a delayed effect on proteinuria, producing a peak reduction on day 7 (56.2±7.6 vs 25.8±4.4 mg/mL, $p < 0.01$) (Fig. 2b).

Effect of malate on renal superoxide dismutase (SOD) and catalase (CAT) activities in UUO-induced nephropathy

Malate elicited a time-dependent increase in SOD activity in the cortex and exerted a peak increase at 180 s (8.7±5.2 vs 0.8±0.4 units/ng, $p < 0.05$) (Fig. 3a). In the medulla, malate tended to increase SOD activity at the same time-dependent fashion in the UUO group ($p > 0.05$) (Fig. 3b). Similarly, malate normalized catalase activity in the cortex of the UUO group, exerting a peak increase at 210 s (0.5±0.1 vs 1.7±0.2 units/ng, $p < 0.01$) (Fig. 3d). Malate significantly increased catalase activity in the medulla of the UUO group, reaching peak levels at 90 s (0.5±0.2 vs 1.4±0.5 units/ng, $p < 0.01$) (Fig. 3c).

Malate modulated L-arginine metabolism in UUO-induced nephropathy

Arginase activity was reduced by 34 % in the cortex of the UUO group and malate significantly restored arginase activity in these animals (0.4±0.1 vs 2.2±0.1 µM/µg, $p < 0.01$) (Fig. 4a). In the medulla, arginase activity increased (~3-fold, $p < 0.01$) compared to sham and treatment with malate further increased this activity in UUO rats (1.7±0.0 vs 2.7±0.4, µM/µg $p < 0.01$) (Fig. 4a). Nitric oxide protects against kidney injury by ensuring renal vasodilation and increased blood flow. As illustrated in Fig. 4b, nitric oxide (NO) production in the cortex of the UUO group was reduced by 25 %, compared to sham ($p > 0.05$), and malate had no significant effect on NO production in the cortex ($p > 0.05$). However, malate significantly increased NO production in the medulla of the UUO group (58.3±1.3 vs 77.8±4.4, µM/ng.

Effect of malate on renal fibrosis in UUO-induced nephropathy

As shown in Figure 5a, collagenase activity in the cortex was not different in the UUO group, compared to the sham, but there was a significant increase in the medulla ($p < 0.05$). Malate significantly increased collagenase activity in the cortex (88.4±2.4 vs 128.2±11.6, µM/mg, $p < 0.05$) in the UUO group, however, collagenase activity significantly reduced in the medulla (149.6±6.1 vs 131.6±4.2, $p < 0.05$) vs UUO group (Fig. 5a). As shown in Figure 5b, in the cortex and medulla of the UUO group, there was an increase in transforming growth factor (TGF-β) expression above vehicle-treated sham levels ($p < 0.05$). Malate tended to increase TGF-β expression in the cortex (22 %, $p > 0.05$) of the UUO group but caused no significant change in the medulla of the UUO group.

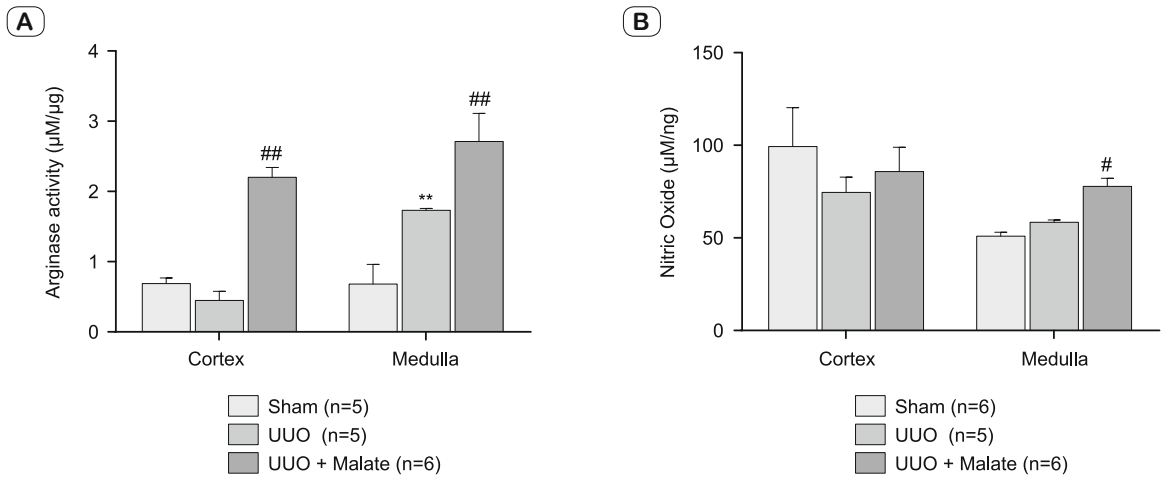

Fig. 4. L-arginine metabolism in obstructive nephropathy. (A) arginase activity and (B) nitric oxide production in rats with UUO-induced renal injury treated with malate (600 mg/kg, po). ** p < 0.01, when compared to sham. # p < 0.05, ## p < 0.01 vs UUO group. Unilateral Ureter obstruction (UUO).

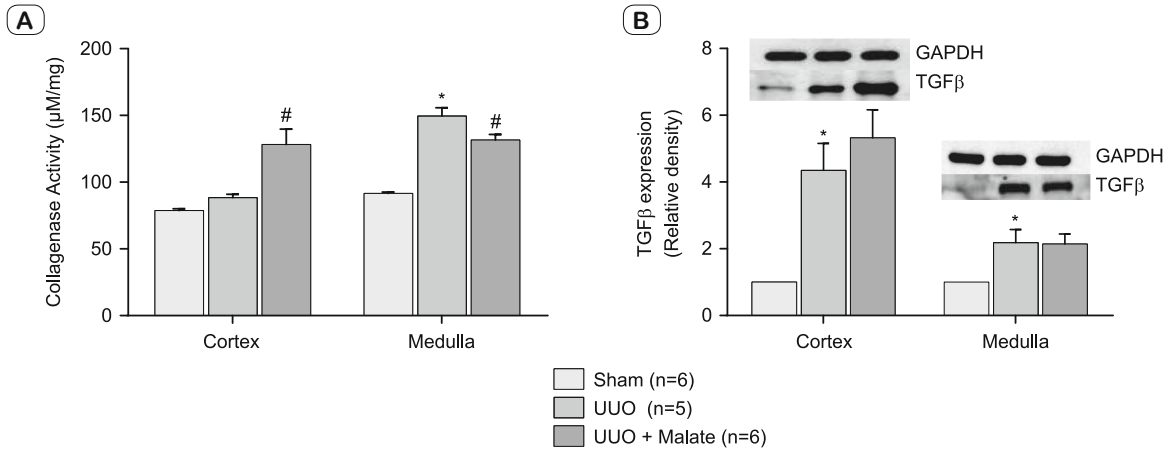

Fig. 5. Renal fibrosis in obstructive nephropathy. Collagenase activity (A) and transforming growth factor (TGF-β) expression (B) in rats with UUO-induced renal injury treated with malate (600 mg/kg, p.o.) for 10 days. * p < 0.05, when compared to sham. # p < 0.05 vs UUO group

Malate upregulated nuclear erythroid factor (Nrf2) expression in UUO-induced nephropathy.

Nrf2, a nuclear transcription factor, stimulates the expression of antioxidant genes to mitigate oxidative stress. As shown in Figure 6, Nrf2 was not different in the cortex and medulla of the UUO group compared to sham ($p > 0.05$). Malate tended to increase Nrf2 expression in the cortex (60 %, $p > 0.05$) and elicited a 2-fold increase in the medulla ($p < 0.05$) of the UUO group.

Discussion

This present study investigated the effects of malate on renal inflammation, L-arginine metabolism, and fibrosis in obstructive nephropathy.

Sodium depletion/wasting occurs in UUO-induced nephropathy due to renal tubular damage. The sodium depletion in obstructive nephropathy was significantly mitigated by malate on days 4 and 7. This decrease in sodium depletion indicates a improvement in renal function (19).

Acute kidney injury (AKI) in obstructive nephropathy is due to the increased expression of the transmembrane protein, kidney injury molecule (KIM-1), that equally serves as an index of early proximal tubule injury (20). KIM-1 expression in the cortex and medulla was significantly elevated in UUO-induced nephropathy. The expression of KIM-1 in the cortex of the UUO group was prominent because of the proximal tubular damage that occurs at an acute stage of UUO-induced nephropathy. Malate significantly reduced KIM-1 expression in the cortex and medulla, indicating that malate attenuated the AKI in obstructive nephropathy. Similarly, malate evoked a late onset decrease in proteinuria, a non-specific renal injury marker, that is directly related to kidney depreciation (21). The actions of malate on KIM-1 expression and proteinuria highlights its ameliorative effect in UUO-induced nephropathy.

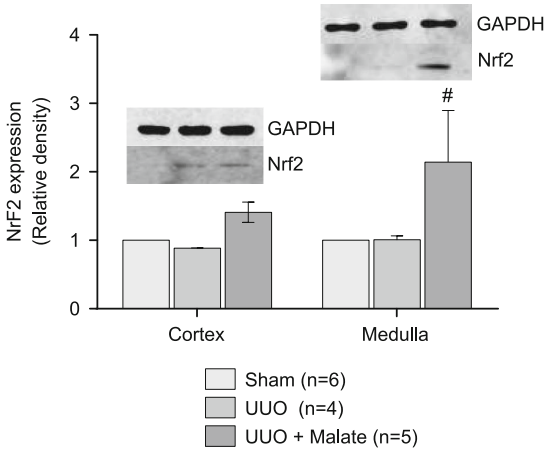

Fig. 6. Nrf2 expression in rats with UUO-induced nephropathy treated with malate (600 mg/kg, po) for 10 days. # p < 0.05 vs UUO group.

Renal inflammation and oxidative stress principally underpin the pathology in UUO-induced nephropathy and the endogenous antioxidant enzymes, especially SOD and CAT, are critical in ameliorating the deleterious effect of inflammation in obstructive nephropathy (22). The activities of these renal antioxidant enzymes are usually reduced in obstructive nephropathy. Consistent with this, data from this study generally revealed low levels of SOD in the cortex of rats with obstructive nephropathy that increased after treatment with malate, indicating a malate-induced reduction in superoxide anion generation. Malate also significantly increased the activity of CAT in the cortex and medulla of UUO. This increase in SOD and CAT activities by malate attenuated the renal inflammation and oxidative stress in obstructive nephropathy. There was also a congruent increase in the expression of the nuclear erythroid factor (Nrf2), a genetic mediator of cell defense response vital for mitigating oxidative stress (23) in the medulla of nephropathic rats treated with malate. This upregulation in Nrf2 expression by malate aligns with the enhanced antioxidant response observed in CAT and SOD studies, thus underscoring that malate exerts antioxidant effects in UUO nephropathy.

L-arginine metabolism, represented by arginase activity and nitric oxide (NO) production, is vital to mitigating UUO-induced nephropathy. NO elicits an increase in renal blood flow, acts as an anti-fibrotic in obstructive nephropathy and is thus, renoprotective (24). Hence, ligands that increase NO generation in obstructive nephropathy could improve its prognosis. This present study showed a reduction in NO in the UUO group that corroborates results from studies by (25) which showed a chronic decrease in NO in UUO. Malate exerted a selective increase of NO in the renal medulla in UUO-induced nephropathy. This increase in NO production protects the vital function of the renal medulla of regulating pressure natriuresis (26) and, by extension, blood pressure and partly underlines the increase in natriuresis, stimulated by malate in obstructive nephropathy (27). There is an inverse relationship between arginase activity and NO production. This present study showed that the increase in arginase activity in the cortex was congruent with the reduced NO production in the renal cortex but not medulla in nephropathic rats treated with malate. The increased arginase activity may have compensatory effects as the increase in ornithine, a by-product of the breakdown of L-arginine by arginase, is needed for cell proliferation and tissue remodeling (28): processes that could improve kidney function in obstructive nephropathy. Hence, the observed renoprotective effect of malate has mechanistic links to NO production and arginase activity.

Renal fibrosis in UUO-induced nephropathy occurs due to an increase in collagen deposition in the interstitial matrix and glomerular basement membrane (29). The activity of collagenase is directly related to its degradation and deposition of collagen (8). Our present study showed a consistent increase in the activity of collagenase in the cortex and medulla of UUO group. This may have resulted in excessive tissue breakdown that worsened renal injury, corroborating earlier reports that documented increased collagenase activity in fibrotic kidneys (29). The treatment with malate paradoxically increased collagenase activity in the cortex but not the medulla of the UUO group. This insinuates that malate could not prevent collagen deposition and by extension, fibrosis in the renal cortex. (30). Cheng et al. provided evidence that collagenase activity correlates with the progression of CKD, and a decrease in collagenase activity may indicate a delay in CKD progression. Hence, the significant lack of collagenase activity in the medulla is thus consistent with this observation. Closely related to collagenase activity is the TGF-β/Smad downstream signal transduction pathway which upregulates the expression of collagenase. TGF-β is a master regulator of fibrosis, hence, modulators of TGF-β downstream effects may be beneficial in ameliorating the UUO-induced renal fibrosis. Contrary to expectation, malate increased TGF-β expression in the cortex but had no effect in the medulla of the UUO group. This observation was consistent with the malate-induced increase in collagenase activity in the cortex but not the medulla, hence, it is likely that the lack of increased TGFβ signaling in the medulla may have also resulted in a lack of collagenase activity. Aside from its profibrotic actions, TGF-β also exerts beneficial and protective effects (31). Smad7, a downstream effector protein of TGF-β inhibits the expression of Nf-κB, a regulator of inflammatory genes that could worsen renal injury. It is thus possible that the paradoxical increase in TGF-β expression in the renal cortex by malate may have an underlying beneficial effect against inflammation and fibrosis.

It is necessary to highlight that malate and its related intermediaries serve as markers of AKI (32). Jan et al (32) reported that due to destruction of cell integrity in renal injury, there was a "leak" of malate from intracellular spaces, causing a deficiency. Hence, it is tenable that the deficiency in the intracellular malate contributed to the pathological consequences of AKI (32). Our present study thus corroborates this notion, particularly as supplementation with malate improved pathological outcomes in nephropathy. It is hoped that further studies would elucidate if deficiencies in these tricarboxylic acid cycle intermediaries could partly underlie the etiology of AKI and CKD.

In conclusion, this study has shown that malate attenuated the renal injury and oxidative stress, but selectively mitigated fi-

brosis in the medulla in obstructive nephropathy. The respective increase in NO production and upregulation of Nrf2 expression underlined the respective renoprotective and antioxidant actions of malate. Thus, malate, the TCA cycle intermediary could ameliorate AKI and improve renal outcomes associated with CKD in obstructive nephropathy.

References

1. Bhatnagar V, Srinivas M. Obstructive Uropathy. In: Pediatric Nephrology. Jaypee Brothers Medical Publishers (P) Ltd.; 2016; 476–476.

2. Hassan NME, Said E, Shehatou GSG. Nifuroxazide suppresses UUO-induced renal fibrosis in rats via inhibiting STAT-3/NF-κB signaling, oxidative stress and inflammation. Life Sci 2021; 23 (272): 11–24.

3. Xiong Y, Chang Y, Hao J, Zhang C, Yang F, Wang Z et al. Eplerenone Attenuates Fibrosis in the Contralateral Kidney of UUO Rats by Preventing Macrophage-to-Myofibroblast Transition. Front Pharmacol 2021; 12 (83): 1-9.

4. Liao Y, Tan RZ, Li JC, Liu TT, Zhong X, Yan Y et al. Isoliquiritigenin attenuates uuo-induced renal inflammation and fibrosis by inhibiting mincle/syk/ nf-kappa b signaling pathway. Drug Des Devel Ther 2020; 14 (3): 1455–1468.

5. Takaori K, Yanagita M. Insights into the Mechanisms of the Acute Kidney Injury-to-Chronic Kidney Disease Continuum. Nephron 2016; 134 (3): 172–176.

6. Martínez-Klimova E, Aparicio-Trejo OE, Tapia E, Pedraza-Chaverri J. Unilateral ureteral obstruction as a model to investigate fibrosis-attenuating treatments. Biomolecules 2019; 9 (4): 1–28.

7. Huang C te, Liu KD. Exciting developments in the field of acute kidney injury. Nat Rev Nephrol 2019; 16 (2): 69.

8. Song J, Xia Y, Yan X, Luo J, Jiang C, Zhang M et al. Losartan accelerates the repair process of renal fibrosis in UUO mouse after the surgical recanalization by upregulating the expression of Tregs. Int Urol Nephrol 2019; 51 (11): 2073–2081.

9. Hou E, Sun N, Zhang F, Zhao C, Usa K, Liang M et al. Malate and Aspartate Increase L-Arginine and Nitric Oxide and Attenuate Hypertension. Cell Rep 2017; 19 (8): 1631–1639.

10. Yang Y, Song M, Liu Y, Liu H, Sun L, Peng Y et al. Renoprotective Approaches and Strategies in Acute Kidney Injury. Pharmacol Ther 2016; 163 (2): 58–68.

11. Kaeidi A, Maleki M, Shamsizadeh A, Fatemi I, Hakimizadeh E, Hassanshahi J. The therapeutic approaches of renal recovery after relief of the unilateral ureteral obstruction: A comprehensive review. Iran J Basic Med Sci 2020; 23 (11): 1367–1376.

12. Edosuyi O, Choi M, Igbe I, Oyekan A. Fumarate exerted an antihypertensive effect and reduced kidney injury molecule (KIM)-1 expression in deoxycorticosterone acetate-salt hypertension. Clin Exp Hypertens 2021; 43 (6): 555–564.

13. Margoshes M, Vallee BL. Flame Photometry and Spectrometry Principles and Applications. In: Methods of Biochemical Analysis 2006; 353–407.

14. Cissell DD, Link JM, Hu JC, Athanasiou KA. A Modified Hydroxyproline Assay Based on Hydrochloric Acid in Ehrlich's Solution Accurately Measures Tissue Collagen Content. Tissue Eng Part C Methods 2017; 23 (4): 243–250.

15. Green LC, Wagner DA, Glogowski J, Skipper PL, Wishnok JS TS. Analysis of nitrate, nitrite, and [15N] nitrate and nitrate in biological fluids. Anal Biochem 1982; 126 (1): 131–138.

16. Iyamu EW, Asakura T, Woods GM. A colorimetric microplate assay method for high-throughput analysis of arginase activity in vitro. Anal Biochem 2008; 383 (2): 332–334.

17. Misra HP, Fridovich I. The Role of Superoxide Anion in the Autoxidation of Epinephrine and a Simple Assay for Superoxide Dismutase the Role of Superoxide Anion in the Epinephrine and a Simple Assay for Superoxide Dismutase. J Biol Chem 1972; 247 (10): 3170–3175.

18. Aebi H. Catalase in vitro. In: Methods in Enzymology. Academic Press; 1984; 121–126.

19. Kinter M, Wolstenholme JT, Thornhill BA, Newton EA, McCormick ML, Chevalier RL. Unilateral ureteral obstruction impairs renal antioxidant enzyme activation during sodium depletion. Kidney Int 1999; 55 (4): 1327–1334.

20. Rizvi MS, Kashani KB. Biomarkers for Early Detection of Acute Kidney Injury. J Appl Lab Med 2017; 2 (3): 386–399.

21. Urbschat A, Obermüller N, Haferkamp A. Biomarkers of kidney injury. Biomarkers 2011; 16 (1): 1–10.

22. Dendooven A, Ishola DA, Nguyen TQ, van der Giezen DM, Kok RJ, Goldschmeding R et al. Oxidative stress in obstructive nephropathy. Int J Exp Path 2011; 92 (3): 202–210.

23. Toth RK, Warfel NA. Strange bedfellows: Nuclear factor, erythroid 2-Like 2 (Nrf2) and hypoxia-inducible factor 1 (HIF-1) in tumor hypoxia. Antioxidants 2017; 6 (27): 1–21.

24. Miyajima A, Chen J, Poppas DP, Vaughan J, Felsen D. Role of nitric oxide in renal tubular apoptosis of unilateral ureteral obstruction. Kidney Int 2001; 59 (4): 1290–1303.

25. Hegarty NJ, Young LS, Kirwan CN, O'neill AJ, Bouchier-Hayes DM, Sweeney P et al. Nitric oxide in unilateral ureteral obstruction: Effect on regional renal blood flow. Kidney Int 2001; 59 (4): 1059–1065.

26. Cowley AW. Role of the renal medulla in volume and arterial pressure regulation. Am J Physiol Regul Integr Comp Physiol 1997; 273 (1): 42.

27. Zou AP, Cowley AW. Role of nitric oxide in the control of renal function and salt sensitivity. Curr Hypertens Rep 1999; 1 (2): 178–186.

28. Gallardo-Soler A, Gómez-Nieto C, Campo ML, Marathe C, Tontonoz P, Castrillo A et al. Arginase I induction by modified lipoproteins in macrophages: A peroxisome proliferator-activated receptor-γ/δ-mediated effect that links lipid metabolism and immunity. Mol Endocrinol 2008; 22 (6): 1394–1402.

29. Rasmussen DGK, Boesby L, Nielsen SH, Tepel M, Birot S, Karsdal MA et al. Collagen turnover profiles in chronic kidney disease. Sci Rep 2019; 9 (1): 1–10.

30. Cheng Z, Limbu MH, Wang Z, Liu J, Liu L, Zhang X et al. MMP-2 and 9 in chronic kidney disease. Int J Mol Sci 2017; 18 (4): 1–11.

31. Sureshbabu A, Muhsin SA, Choi ME. TGF-β signaling in the kidney: profibrotic and protective effects. Amer J Physiol – Renal Physiol 2016; 310 (7): 596–606.

32. Jan HAL, Nielsen PM, Eldirdiri A, Bertelsen LB, Joørgensen HS, Laustsen C. Fumarase activity: An in vivo & in vitro biomarker for acute kidney injury. Sci Rep 2017; 7 (9): 1–10.

Received September 8, 2022.
Accepted September 21, 2022.